Ocean Dynamics (2023) 73:575–591
https://doi.org/10.1007/s10236-023-01570-y

Evaluation of the applicability of the Ekman theory for wind-driven ocean currents: a comparison with the Mellor–Yamada turbulent model

Tal Ezer[1]

Received: 23 May 2023 / Accepted: 7 August 2023 / Published online: 29 August 2023

Abstract
The classical Ekman theoretical solution for steady-state wind-driven currents of homogeneous ocean with constant eddy viscosity was obtained more than a century ago. However, it is not clear how applicable this solution is for realistic stratified ocean with depth-dependent turbulent mixing coefficient (KM). In this study, the Ekman analytical solution is compared with currents obtained by one-dimensional Mellor–Yamada turbulent ocean model (1D-MY) to assess the accuracy of the Ekman solution under various oceanic conditions. For experiments with constant density but depth-dependent KM, the Ekman solution is close to the 1D model calculation if the analytical solution uses the mean KM obtained by the 1D model for each wind speed. Inclusion in the 1D-MY model, the Craig–Banner (C-B) turbulence induced by surface breaking waves makes the surface velocity in the model more like the Ekman surface velocity; however, C-B mixing only affects current direction and speed of the upper ~ 5 m and only for strong winds. Model experiments with different mixed layer (ML) depths show abrupt decline in turbulence and vanishing currents below the ML, so model currents below the ML are weaker than the Ekman solution for an unstratified ocean. The best comparison between the model and the Ekman solutions was found when the Ekman equations use mean KM calculated from the model over the ML depth plus 10 m of the thermocline below. Sensitivity model experiments with different winds and different stratifications resulted in an empirical formula that estimates the mean KM from observed wind and ML depth, and this relation can complement the classical Ekman formula in cases where KM is unknown.

Keywords Ekman transport · Turbulence · Mellor–Yamada scheme · Mixed layer

1 Introduction

The wind-driven ocean currents and related circulation patterns have been of great interest for a long time (Munk 1950), and one of the pioneering findings to understand these processes was the theoretical work by Ekman (1905). Ekman recognized the important impact on upper ocean wind-driven currents from Earth rotation (i.e., the Coriolis effect) and oceanic turbulence. The turbulent mixing in his model was represented by an eddy viscosity coefficient (marked hereafter as KM). For a homogeneous ocean with constant KM, an analytical steady-state solution for the equations of motion can be found if KM, wind stress, and latitude are known. The solution is the so-called Ekman spiral where currents in the northern hemisphere turn to the right with depth and decay exponentially within the so-called Ekman layer, resulting in "Ekman transport" that is directed 90° to the right of the wind direction; the vertically integrated transport over the Ekman layer depends only on wind stress and Coriolis, but the Ekman layer depth depends also on the eddy viscosity coefficient. Variations of the Ekman theory can be found in several studies; for example, Wang et al. (2003) found solution that includes time-dependent terms and bottom slope. Note that bottom friction stress can create a similar bottom Ekman layer, where currents turn with depth in opposite direction to the surface currents (e.g., Wang et al. 2003; Ezer 2005); here, only the surface Ekman layer is studied. The Ekman theoretical solution is now an integral part of

Topical Collection of the 13th International Workshop on Modeling the Ocean (IWMO), Hamburg, Germany, 27-30 June 2023.

This is an original research that has not been submitted or under consideration for any other publication.

✉ Tal Ezer
tezer@odu.edu

[1] Center for Coastal Physical Oceanography, Old Dominion University, 4111 Monarch Way, Norfolk, VA 23508, USA

every physical oceanography textbook (e.g., Pond and Pickard 1983; Mellor 1996). The shortcoming of the Ekman solution is that KM is unknown and can vary by several orders of magnitude in space, time, and depth, and moreover, the upper ocean is mostly stratified and subject to time variations in wind and heat exchange with the atmosphere, so attempts to verify the Ekman theory with observations are often inconclusive (Price et al 1987). Nevertheless, analysis of observations of the upper ocean currents by Price et al. (1987) found that the total Ekman transport is within ~ 10% of the theoretical solution, though the actual current structure in a stratified ocean is much more complex than the Ekman theory predict. Laboratory experiments can also demonstrate the basic idea behind the Ekman theory but only qualitatively (Beesley et al 2008). Attempts to improve the classical theory and develop turbulent Ekman theory with depth and time-dependent KM that also includes wave mixing have been tried as well, but they are complicated and may be difficult to verify with observations (Huang 1979). Gaspar et al. (1990) show that a simple diagnostic eddy mixing model can produce currents that qualitatively resemble the theoretical Ekman spiral and agree quite well with observations.

The above studies motivated us to conduct experiments that systematically and quantitatively aim to evaluate the Ekman solution against one-dimensional prognostic numerical ocean model with the Mellor–Yamada turbulent scheme (M-Y, Mellor and Yamada 1982; Mellor 2001); the M-Y scheme is similar to the code used, for example, by the three-dimensional Princeton Ocean Model (POM, Blumberg and Mellor 1987), as well as other community ocean models. The goal is to assess how factors that have been ignored in the Ekman model, such as non-constant KM and stratification, may affect the solution and possibly lead to modification of the Ekman solution so it can be applied to more realistic ocean conditions.

Note that the original M-Y model itself, when compared with observations, has its own drawbacks such as underrepresentation of mixing under strong summer stratification (i.e., Martin 1985). Therefore, numerous studies attempted to improve the M-Y model or add additional mixing due to surface or internal waves (Galperin et al 1988; Craig and Benner 1994; Mellor and Blumberg 2004; Stacey and Pond 1997; Ezer 2000; Mellor 2001; Huang et al 2011). Improving the M-Y model itself is beyond the scope of this study. However, some experiments with surface wave mixing by Craig and Benner (1994) (C-B), and Stacey and Pond (1997) as used by Mellor and Blumberg (2004), were conducted to test the impact of waves on the surface currents. Here, only the enhanced mixing due to surface waves breaking is considered, not the nonbreaking waves impact such as in Huang et al (2011) and others. As indicated by numerous past studies, it is difficult to compare the Ekman theoretical solution with observations, since the real ocean includes non-wind-driven components such as geostrophic and tidal currents, which can be larger than the pure wind-driven currents. Moreover, stratification can significantly affect the currents, making them more surface trapped within the mixed layer (ML) and thus diverge from the classical Ekman spiral — this has been shown, for example, by a simple surface ML model (Price et al 1987). The experiments conducted here thus allow us to focus only on wind-driven ocean currents in a controlled idealized model setting, but unlike some past studies with ML models, the Ekman theory is compared here with a model that includes depth-dependent eddy mixing coefficients based on a full column turbulent model.

It is important to note that better understanding of turbulent processes in the upper ocean and finding ways to quantify turbulent mixing coefficients may be vital to some biological processes such as particulate organic carbon transport from the upper ocean to the mesopelagic zone with potential role played by the mixed layer biological pump (Dall'Olmo et al. 2016; Lacour et al 2019). The strength of Ekman upwelling which is essential for biological productivity (McClain and Firestone 1993; Jacox et al 2018) may also depend on turbulent processes of the upper layers which are not always well-known. However, in the context of the 1D model used here where horizontal gradients and horizontal advection are neglected, Ekman transport-driven upwelling near coasts and Ekman pumping due to wind stress curl are not part of the solution.

The paper is organized as follows. First, the Ekman solution is briefly described in Section 2, and then the turbulent model and the experiments are described in Section 3. Results in Section 4 include simulations without stratification and then simulations with different mixed layer depths. Section 5 is a summary and conclusion.

2 The Ekman spiral and Ekman layer

The classical Ekman theory (Ekman 1905) of wind-driven currents $[u(z), v(z)]$ under constant wind stress (τ_x, τ_y) in a homogeneous ocean assumes a momentum balance between the Coriolis acceleration and vertical eddy viscosity:

$$-fv = KM\frac{\partial^2 u}{\partial z^2}, fu = KM\frac{\partial^2 v}{\partial z^2}, \quad (1a,b)$$

where KM is assumed to be a constant (unknown) vertical eddy mixing coefficient and $f = 2\Omega\sin(\lambda)$ is the Coriolis parameter for latitude λ and $\Omega = 7.3\times10^{-5}$ s^{-1} is the angular velocity of Earth rotation. For simplicity, the classical steady-state solution in most textbooks (e.g., Pond and Pickard 1983; Mellor 1996) often assumes a constant wind from the south, but here, an eastward blowing wind is assumed (for esthetic reason, plots of the two velocity components are shown more clearly when they have opposite sign), so the surface wind stress is

$$\tau_x = -\frac{\rho_{air}}{\rho_{\text{water}}}C_D U^2, \tau_y = 0 \quad (2a,b)$$

where the ratio between air and water densities is taken as 1.2×10^{-3} and a constant drag coefficient $C_D = 1.2\times10^{-3}$ was used, which is a reasonable value for U = 5–10 m/s winds (Garratt 1977). Note that this is the kinematic wind stress force (in m^2/s^2) on the ocean side. Also, since both the Ekman theoretical solution and the numerical model (see later) use the same formula, adjusting C_D to a more accurate non-constant value would not affect the main results. Under these conditions, the Ekman solution is

$$u = Acos\left(\frac{-\pi}{4}+\frac{\pi}{D_E}z\right), v = Asin\left(\frac{-\pi}{4}+\frac{\pi}{D_E}z\right), \quad (3a,b)$$

where the amplitude (A) depends on the surface current speed (V_0), on the Ekman layer depth (D_E), and decays exponentially with depth (here $0 > z > -50$ m)

$$A = V_o e^{\frac{\pi}{D_E}z}, V_o = \frac{|\tau_x|}{\sqrt{KM|f|}}, D_E = \pi\sqrt{\frac{2KM}{|f|}}. \quad (4a,b,c)$$

Therefore, for a given latitude (λ), wind speed (U), and eddy mixing coefficient (KM), the Ekman velocities [$u(z)$, $v(z)$] can be calculated by Eqs. 2–4. In the experiments conducted here, latitude was fixed at λ = 30°N, while constant wind of different strength, 2 m/s < U < 15 m/s, was used in each experiment. Experiments (not shown) with different latitudes did not have significant impact on comparisons between the theoretical Ekman solution and the numerical model, as they both use the same Coriolis parameter. The turbulent mixing coefficient used in Eq. (4) was based on vertical averaged values obtained from the 1D model results (see below), with typical values of $5 < KM < 500 cm^2/s$, depending on each case. Note that while the equations above used meters, for clearer presentation, current velocity and KM are shown in cm/s and cm^2/s, respectively ($1\ cm^2/s = 10^{-4}\ m^2/s$).

3 The one-dimensional Mellor–Yamada turbulent model

One-dimensional modeling of vertical mixing in the upper ocean based on turbulent theories and models has a long history (Mellor and Durbin 1975; Huang 1979; Martin 1985; Gaspar et al. 1990; Noh and Kim 1999; Mellor 2001; Mellor and Blumberg 2004; Choi et al 2022). Here, the so-called Mellor–Yamada (M-Y) level 2.5 turbulent model was used (Mellor and Yamada 1982) with some experiments adding the Craig–Banner (C-B) (Craig and Banner 1994) surface wave enhanced mixing with boundary condition by Stacey and Pond (1997), as implemented by Mellor and Blumberg (2004). Observations by Price et al. (1987) found that with weak or no stratification, the Ekman layer depth affected by wind stress extends to about 50 m (and less for stratified ocean with a mixed layer), so the model is set to simulate the upper 50 m using 100 vertical layers with higher resolution near the surface (~0.05 m) and lower in the deeper depths (~0.52 m). The model started from different initial temperature profiles (salinity is constant) is executed for 6 days with a time step of 5 min and output saved every 3 h.

The numerical model solves the time-dependent momentum and temperature equations:

$$\frac{\partial u}{\partial t} - fv = \frac{\partial}{\partial z}\left(KM\frac{\partial u}{\partial z}\right), \frac{\partial v}{\partial t} + fu = \frac{\partial}{\partial z}\left(KM\frac{\partial v}{\partial z}\right), \frac{\partial T}{\partial t} = \frac{\partial}{\partial z}\left(KH\frac{\partial T}{\partial z}\right), \quad (5a,b,c)$$

where the vertical eddy diffusivities for momentum (KM) and heat (KH) in the M-Y model are

$$KM = qlS_M, KH = qlS_H \quad (6a,b)$$

S_M and S_H are stability factors that are function of the Richardson number, $q^2/2$ is the turbulent kinetic energy, and l is the turbulent length scale. q and l in M-Y level 2.5 model are solved by two prognostic equations (e.g., see Mellor 2001). In the original M-Y model, the surface boundary condition (at z = 0) was $q = 0$, but in experiments that include the C-B enhanced wave mixing (Craig and Banner 1994), the boundary condition was changed to

$$K_q\frac{\partial q^2}{\partial z} = 2\alpha_{CB}|\tau|^{3/2}, \quad (7)$$

where $K_q = 0.41K_H$, the C-B constant $\alpha_{CB} = 100$, and $|\tau| = \sqrt{\left(\tau_x^2+\tau_y^2\right)}$. Mellor and Blumberg (2004) show that Eq. (7) can reduce warm model bias during summer, but the results were not very sensitive to α_{CB} value between 50 and 100 and affected mostly the near-surface layers. To our knowledge, no previous study quantified if and how the C-B scheme may affect Ekman velocities, but studies with formulations similar to 7 showed, for example, the importance of wind-wave mixing for simulating realistic flows in places like the Bering Sea (Hu and Wang 2010).

A series of sensitivity experiments were conducted with different stratification, different wind speeds, and different turbulent calculations (with and without the C-B scheme); the experiments are summarized in Table 1. Figure 1 shows examples of model calculations with initial condition of a linear temperature profile where T changed from 27 °C at the surface to 20 °C at 50 m. Note that in all these short-term calculations, surface heat flux was neglected, though it can easily be added to simulate the seasonal ML (Ezer 2000). With a constant wind of 10 m/s blowing for 6 days (ramped up over first day to

Table 1 Summary of the experiments with the 1D turbulent numerical model. All simulations were for 6 days (most results are shown at the end of the run) with constant wind blowing eastward and temperature T(z) fixed in time (temperature was allowed to change only in the test case shown in Fig. 1, which is not included in the table); salinity was constant S = 35ppt. The turbulent coefficient KM(z) was either held constant (case 1), calculated by the Mellor–Yamada model ("M-Y"; cases 2–7, 14–21), or calculated by the Mellor–Yamada model with Craig–Banner wave mixing ("C-B"; cases 8–13). Stratification is only included in cases 14–21)

Experiment	Temperature (T, °C)	ML depth (D, m)	Wind speed (U, m/s)	Turbulent coefficient (KM, cm^2/s)
1. KM50-U10	27	> 50	10	50
2. KMMY-U02	27	> 50	2	M-Y
3. KMMY-U05	27	> 50	5	M-Y
4. KMMY-U07	27	> 50	7.5	M-Y
5. KMMY-U10	27	> 50	10	M-Y
6. KMMY-U12	27	> 50	12.5	M-Y
7. KMMY-U15	27	> 50	15	M-Y
8. KMCB-U02	27	> 50	2	C-B
9. KMCB-U05	27	> 50	5	C-B
10. KMCB-U07	27	> 50	7.5	C-B
11. KMCB-U10	27	> 50	10	C-B
12. KMCB-U12	27	> 50	12.5	C-B
13. KMCB-U15	27	> 50	15	C-B
14. MY-U05-D10	20–25.6	10	5	M-Y
15. MY-U10-D10	20–25.6	10	10	M-Y
16. MY-U05-D20	20–24.2	20	5	M-Y
17. MY-U10-D20	20–24.2	20	10	M-Y
18. MY-U05-D30	20–22.8	30	5	M-Y
19. MY-U10-D30	20–22.8	30	10	M-Y
20. MY-U05-D40	20–21.4	40	5	M-Y
21. MY-U10-D40	20–21.4	40	10	M-Y

reduce inertial oscillations), a near steady state is established with a ML of ~ 20 m thickness and surface temperature that cooled by ~ 1.5 °C from its initial condition (Fig. 1a, e). At the end of the run, the turbulent mixing in the M-Y model is maximum at ~ 8 m depth and limited to the ML (Fig. 1c, f). When the C-B wave mixing is added, a significantly larger eddy mixing is seen in the upper 5 m (Fig. 1d). However, the temperature after 6 days was not significantly affected by the wave mixing (Fig. 1b) since the mixed layer depth due to wind-driven turbulence already reached a deeper depth than the depth influenced by surface wave breaking.

4 Results

4.1 Experiments with no stratification

The simplest test of the numerical model is to see how well it can reproduce the Ekman flow under similar condition as the Ekman assumptions in Eq. (1), i.e., a constant temperature and a constant KM (i.e., the model skips Eq. 5c and replaces Eq. 6a, b with a constant value). In this example, KM = 50 cm^2/s and U = 10 m/s (experiment KM50-U10 in Table 1). The results compare the analytical Ekman solution (Eq. 3a, b) with the numerical model solution (Eq. 5a, b) and are shown in Fig. 2. Note that because the velocities of the two solutions are so similar, it is difficult to distinguish between them (blue and red lines in Fig. 2a, b). In this case, the model shows the classical Ekman spiral with surface currents 45° to the right of the wind and turning with depth; in the upper 30 m, the difference between the two solutions is < 0.1 cm/s in speed and < 1° in direction. Note also that at deeper layers where velocity is close to zero, current direction is meaningless, so it is not plotted. While this test is quite trivial, it is important to show that there are no significant numerical errors in the model due numerical instabilities, the finite differencing scheme, or the grid size, before advancing to more complex cases.

In the next two experiments (KMMY-U05 and KMMY-U10; Table 1), density remains constant (T = 27 °C, S = 35ppt) throughout the 50 m model depth, but the constant KM of the previous case is replaced by turbulent mixing from the M-Y model under 5 m/s and 10 m/s winds and shown in Fig. 3 and Fig. 4, respectively. Note that below ~ 20 m, spurious KM may appear in the model without stratification since $\partial\rho/\partial z = 0$ and $\partial u/\partial z \sim \partial v/\partial z \sim 0$, so the Richardson number is not clearly defined; this however, has no impact on the deep velocity (which is near zero) and the temperature (which is held constant). After a few spurious points are removed, the mean KM is calculated (shown as vertical dash line in Fig. 3f). In the Ekman calculation without stratification, the mean model KM over the entire water column is used in Eq. 4. In those two simulations, the model surface current is larger by ~ 5 and ~ 10 cm/s than the Ekman solution for MY-5 and MY-10, respectively, and the surface current direction in the model is closure to the wind direction than the Ekman flow is. However, below the upper ~ 2 m, the difference in velocity between the

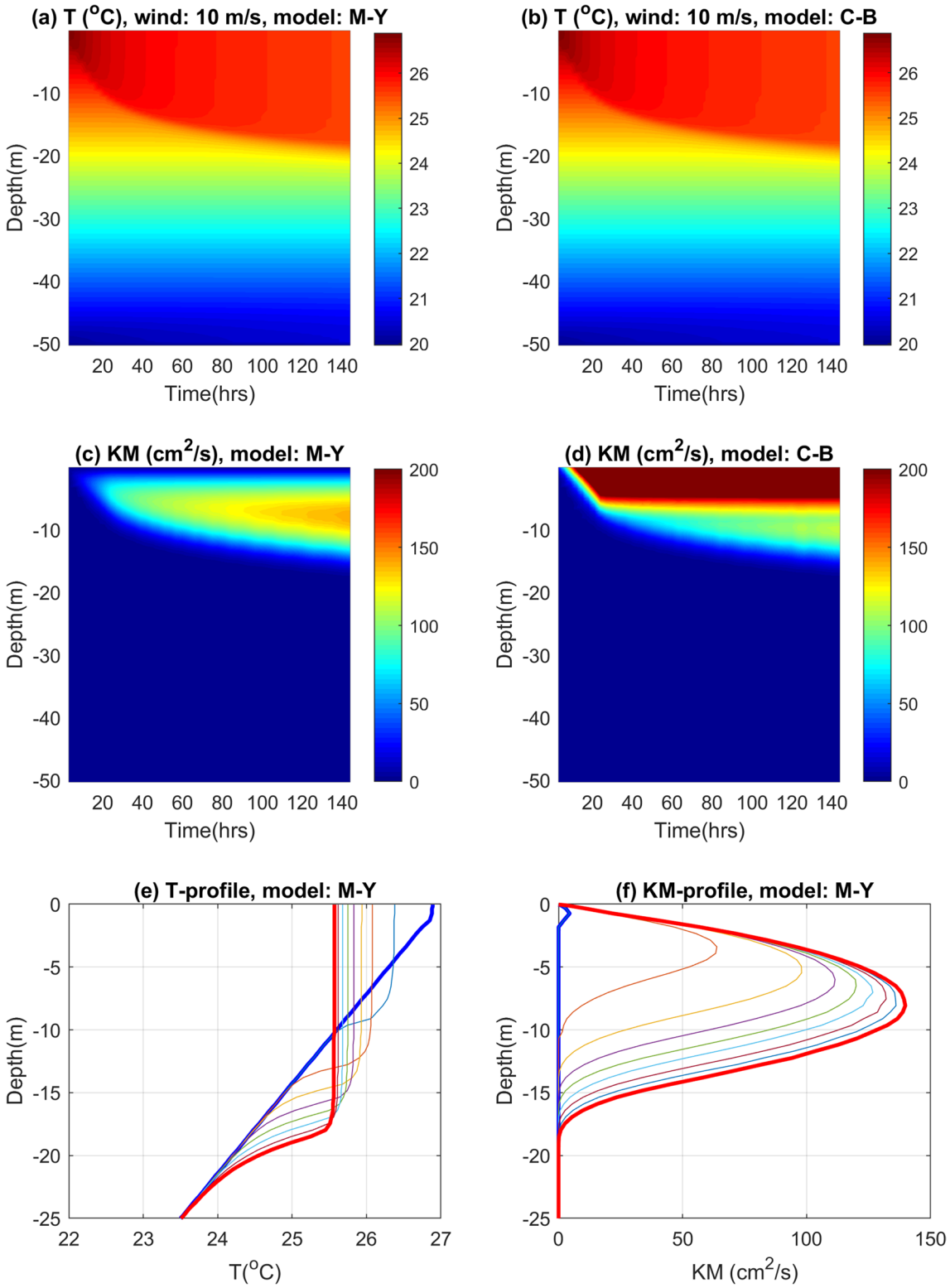

Fig. 1 Examples of 6-day simulations with the 1D model and the development of a mixed layer from linear initial stratification under 10 m/s wind. **a** and **c** are temperature (T) and mixing coefficient (KM) using the Mellor–Yamada (M-Y) model, while **b** and **d** are the same plots when Craig–Banner (C-B) wave mixing is added to the M-Y model. **e** and **f** are the vertical profiles of T and KM in the upper layers every 18 h in the M-Y case; blue and red heavy lines represent profiles near the beginning and end of the runs, respectively

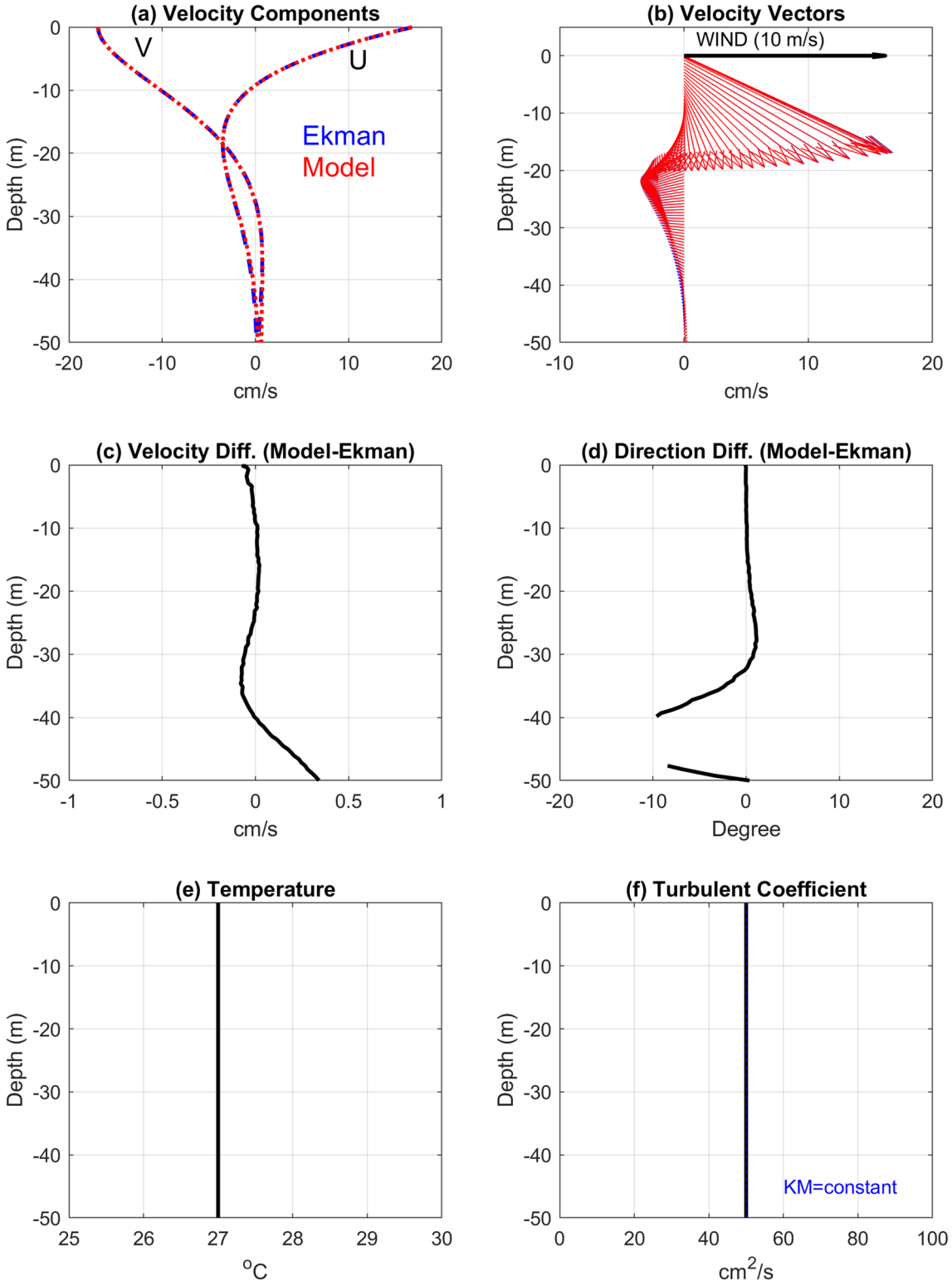

Fig. 2 Simulations with constant T (**e**) and constant KM (**f**) under 10 m/s constant eastward wind (case 1 in Table 1). **a** and **b** are the velocity components and current vectors, respectively, obtained from the Ekman formula (blue) and the M-Y model (red). **c** and **d** are the differences between the two calculations for velocity speed and direction, respectively. Direction is not calculated for velocities close to zero (< 0.2 cm/s). Note that the surface current direction in **b** is 45° relative to the wind, though the *x*-axis is stretched to show more details

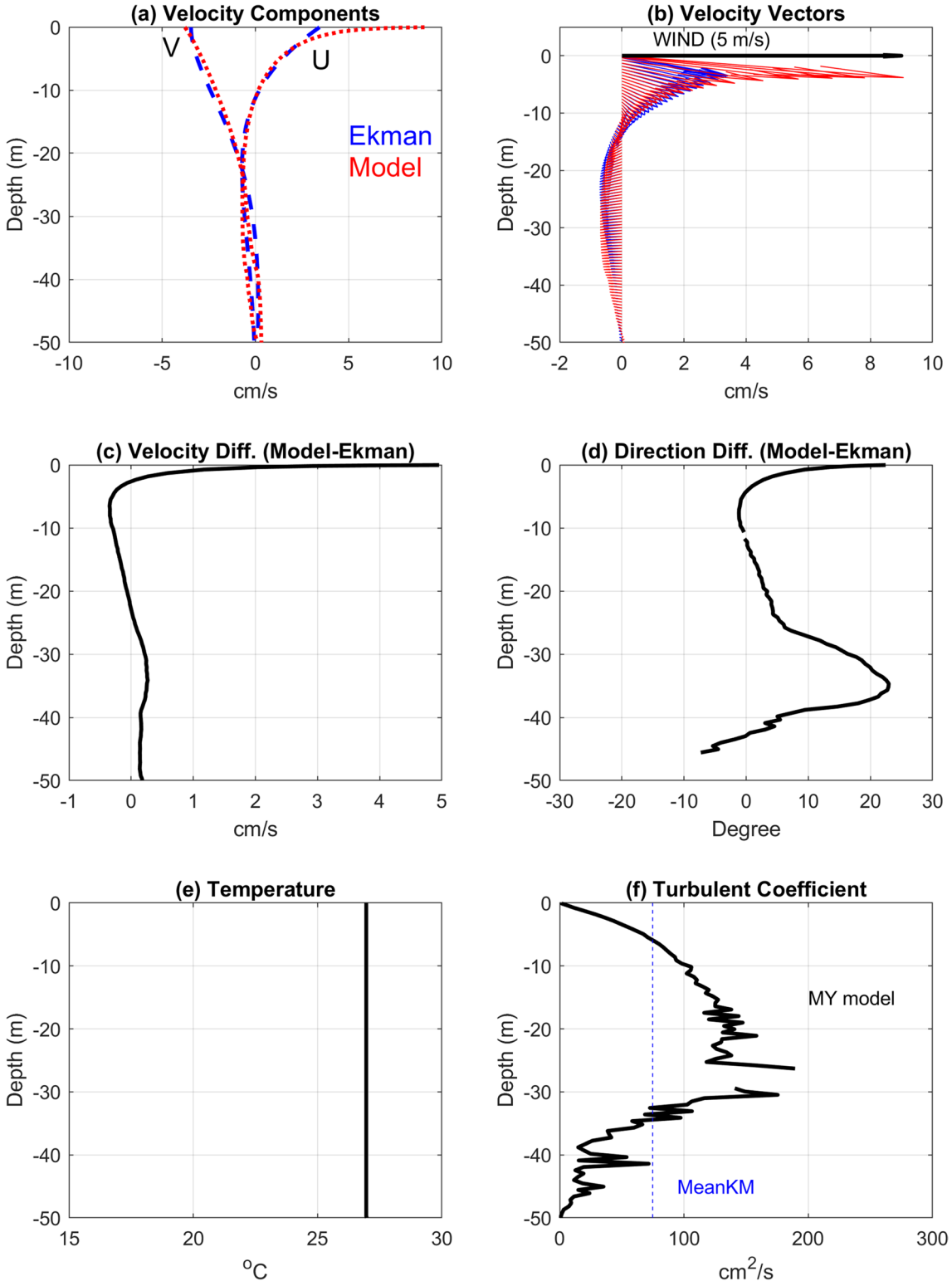

Fig. 3 Same as Fig. 2 but for 5 m/s wind and depth-dependent KM (case 3 in Table 1). KM in the M-Y model is shown in **f**, while the Ekman formula uses the mean KM (vertical dashed blue line). Spurious model KM when velocities are near zero were removed

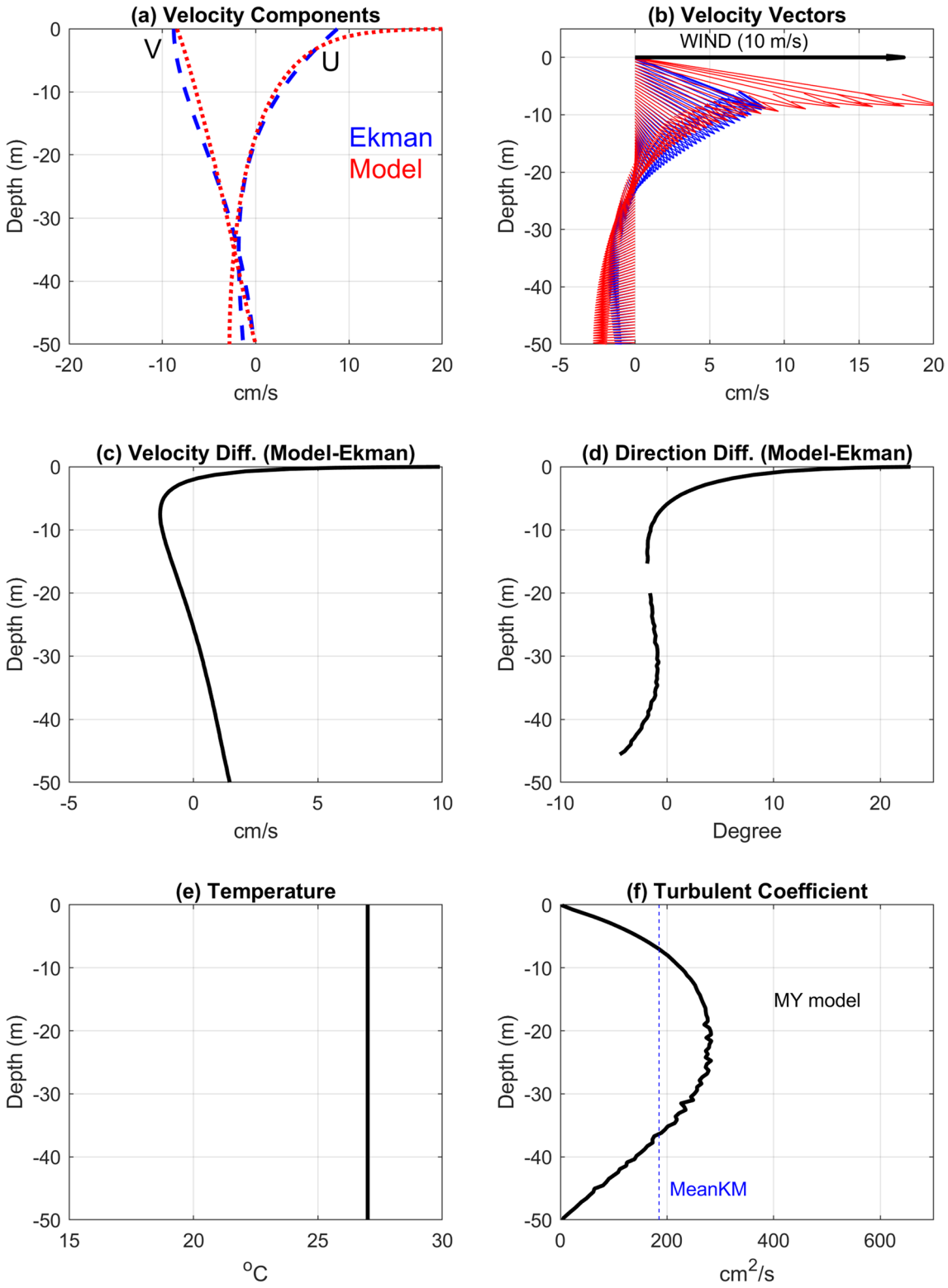

Fig. 4 Same as Fig. 3, but for 10 m/s wind (case 5 in Table 1)

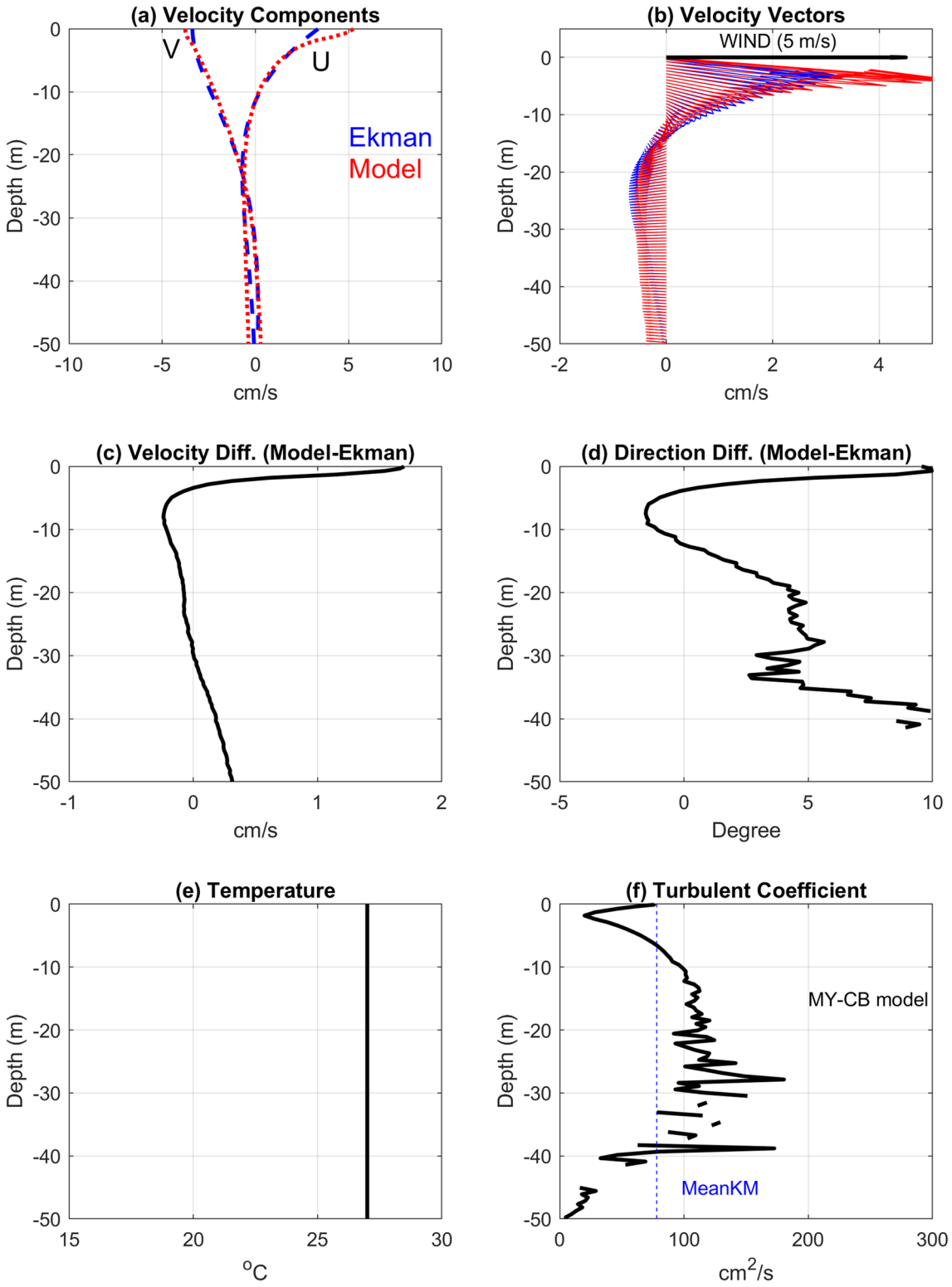

Fig. 5 Same as Fig. 3 (5 m/s wind), but for M-Y model with C-B wave mixing added (case 9 in Table 1)

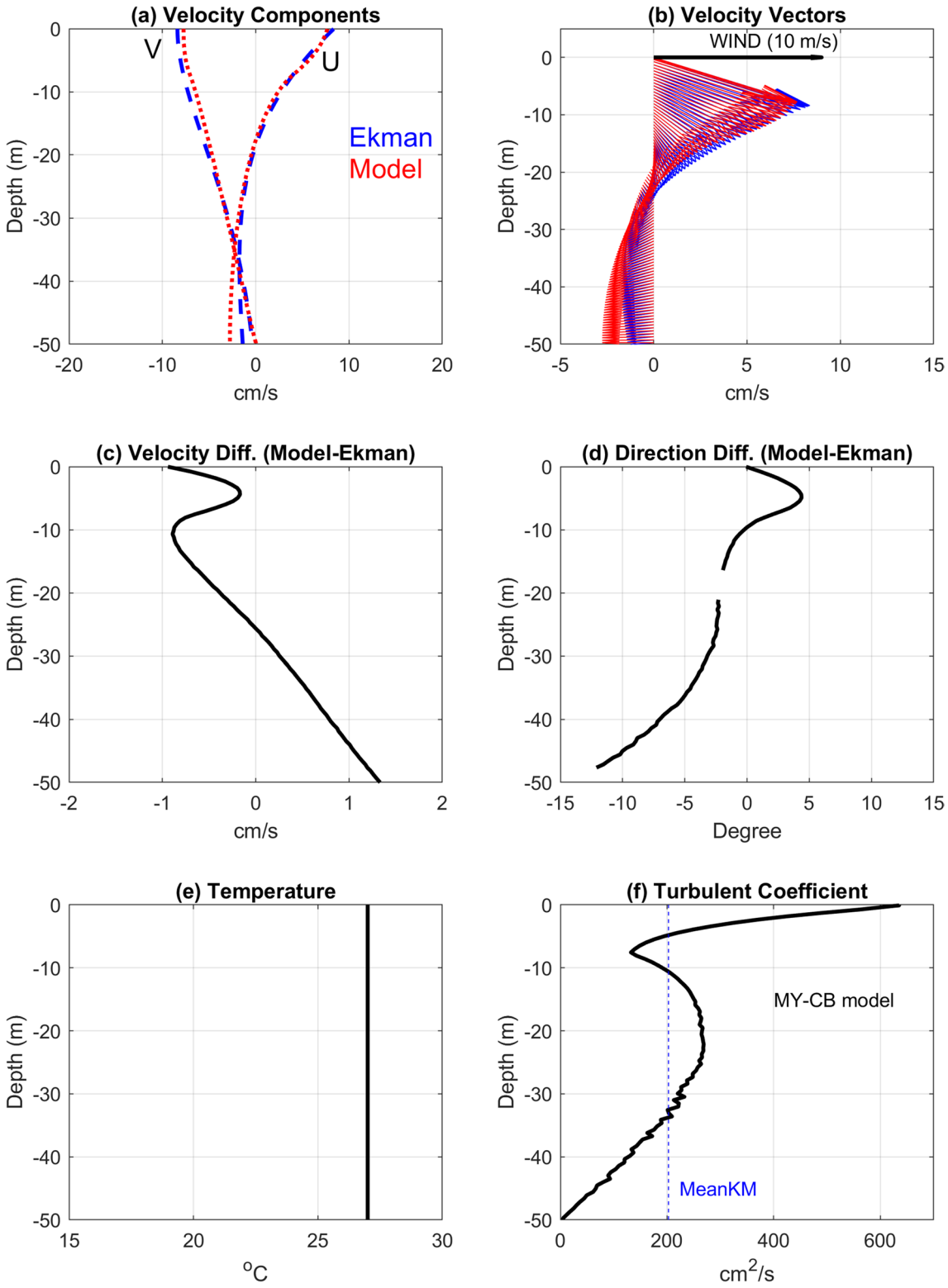

Fig. 6 Same as Fig. 4 (10 m/s wind), but for M-Y model with C-B wave mixing added (case 11 in Table 1)

Ekman and model solutions is quite small (<0.5 cm/s) and likely below observational errors (Price et al 1987).

In the next two experiments (KMCB-U05 and KMCB-U10; Table 1), the boundary condition of the turbulent mixing of the M-Y model uses the C-B surface condition that includes enhanced wave mixing (Eq. 7), and the results are shown in Fig. 5 and Fig. 6, for U = 5 m/s and 10 m/s, respectively (to be compared with Fig. 3 and Fig. 4). The wave mixing effect is especially apparent in the case with strong winds where surface KM increased to over 600 cm^2/s (Fig. 6f). Surface wave breaking mixing reduces the difference between the Ekman and the model surface currents from ~5 to <2 cm/s for 5 m/s wind (Fig. 3c and Fig. 5c) and from ~10 to ~1 cm/s for 10 m/s wind (Fig. 4c and Fig. 6c). Note that because the wave mixing only affects a very thin surface layer (~2–5 m), the mean KM used in the Ekman solution has not changed much from the original M-Y mean KM. The results demonstrate that the Ekman veering in the model is affected by surface turbulence under strong winds and in the C-B model with 10 m/s wind the surface current direction is almost identical to the theoretical Ekman flow.

Additional experiments with both M-Y and C-B models were conducted for different winds ranging from 2 to 15 m/s (experiments 2–13 in Table 1), and the results are summarized in Fig. 7. The wave-induced mixing (C-B) seems to affect the averaged eddy mixing coefficient KM only for wind speeds larger than ~10 m/s (Fig. 7a). The mean KM in the M-Y cases increases linearly with wind speed (blue line in Fig. 7a); thus, if one wants to use the Ekman equations (Eqs. 3 and 4) to calculate the currents when there is no stratification in the upper 50 m, an estimated formula for the cases tested here would be

$$KM\left(\frac{cm^2}{s}\right) = 22U\left(\frac{m}{s}\right) - 37, 2m/s < U < 15m/s. \quad (8)$$

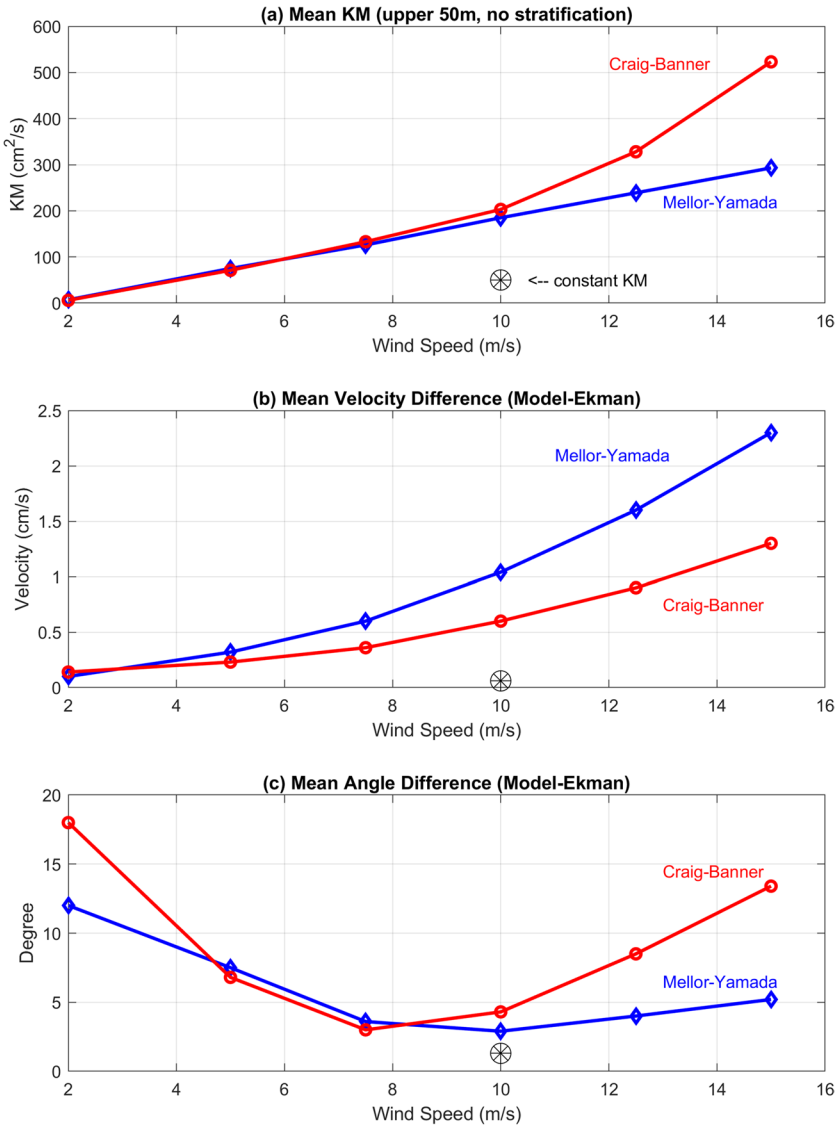

Fig. 7 **a** Mean KM of the upper 50 m as a function of wind for the M-Y (blue) and C-B (red) models without stratification (cases 2–13 in Table 1). **b** and **c** are the differences between the models and the Ekman solutions for current velocity and direction, respectively. Also shown is the value for the constant KM simulation in Fig. 2 (case 1 in Table 1)

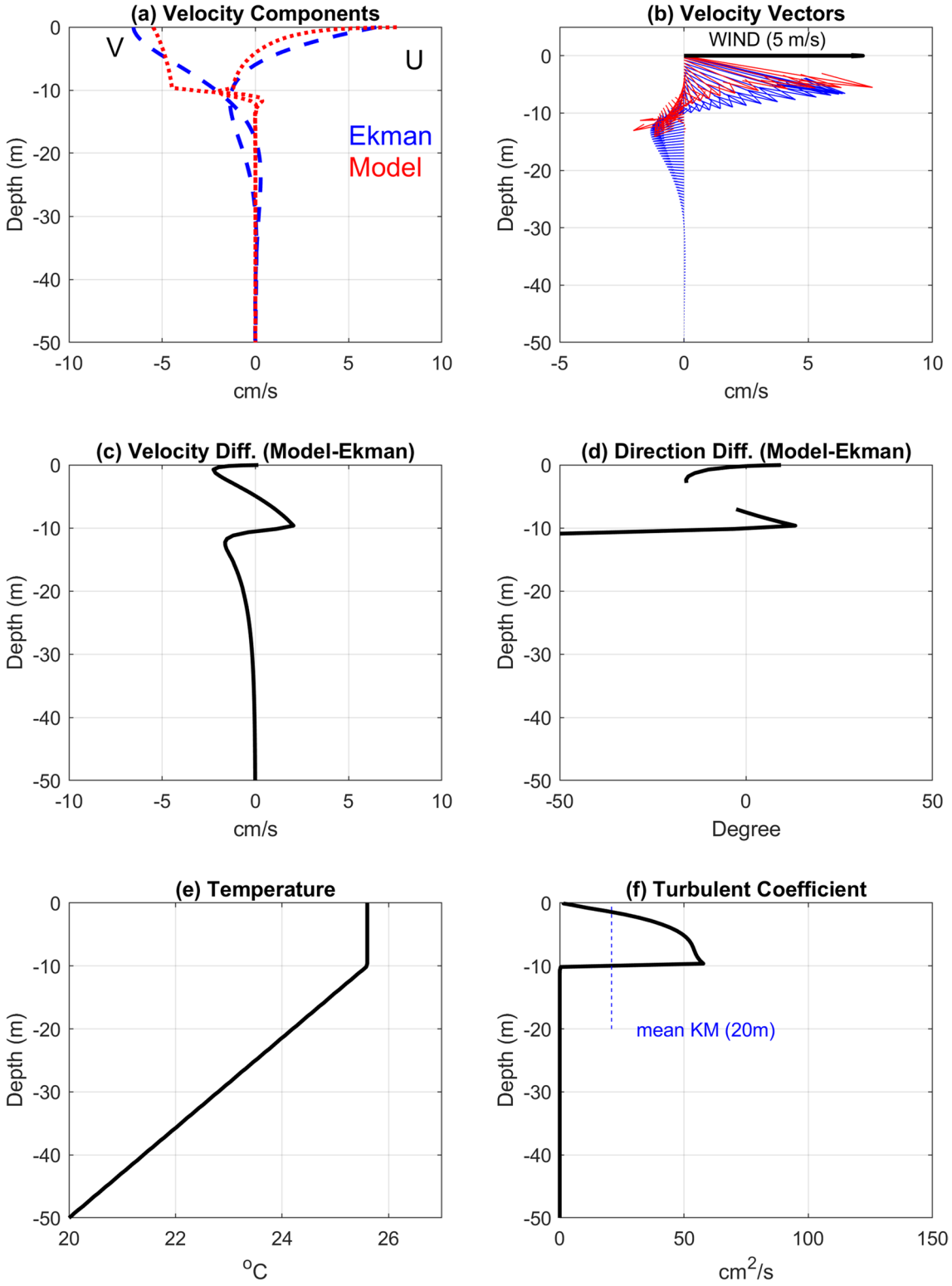

Fig. 8 Same as Fig. 3 (5 m/s wind, M-Y model), but with stratification that includes 10 m deep mixed layer (case 14 in Table 1). The mean KM (**f**) used for the Ekman formula is averaged over the mixed layer depth plus 10 m

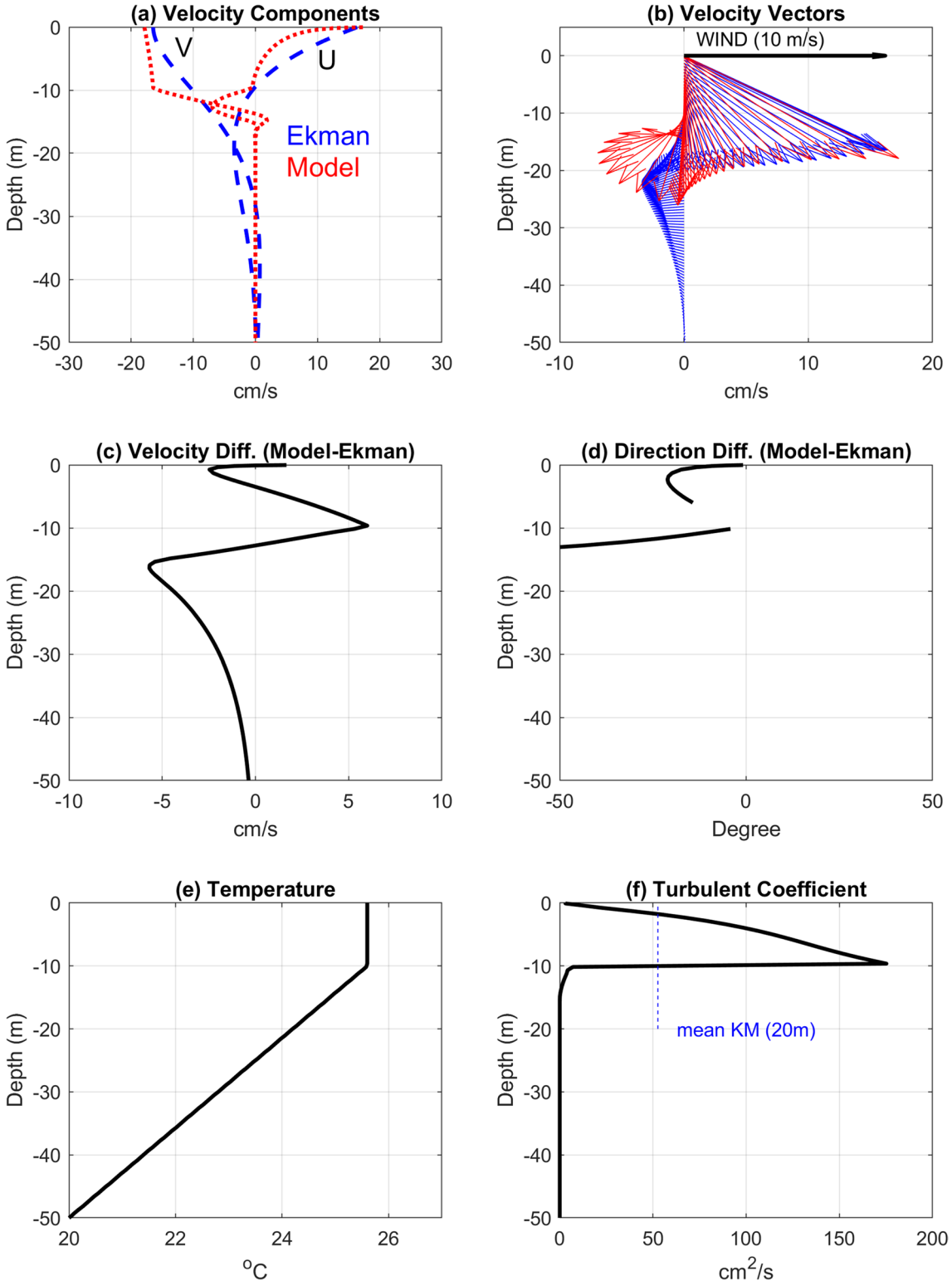

Fig. 9 Same as Fig. 8, but for 10 m/s wind (case 15 in Table 1)

The mean difference in velocity between the Ekman and the model solutions (Fig. 7b) is quite small (< 1 cm/s for winds below 10 m/s), but the difference increases with wind speed and is smaller for the C-B cases. The difference is only relatively larger in the upper 2–5 m in the cases with no wave mixing. However, one should keep in mind that observations and models often do not resolve the fine structure very close to the surface. The overall difference between the Ekman and model solutions in current direction (Fig. 7c) shows that despite the improved surface currents in the C-B model relative to M-Y, over the entire 50 m water column, the M-Y model has slightly better results than C-B, especially for very weak or very strong winds. This can be seen, for example, in Fig. 6d, where the C-B model provides a perfect match of current direction at the surface, but larger departure from the Ekman solution at depth.

4.2 Experiments with stratified ocean and a mixed layer (ML)

As shown by observations and models (Mellor and Durbin 1975; Martin 1985; Price et al 1987; Ezer 2000), the turbulence in a stratified ocean is very different than in the homogeneous water column as assumed by the Ekman theory. The surface ML depth and thermocline strength can change daily and seasonally, whereas stable stratification below the ML would limit wind-driven turbulent mixing at depth (potential deep mixing by internal tides, internal waves, or interaction with bottom topography is neglected here). Therefore, 8 additional experiments with the M-Y model were conducted (experiments 14–21 in Table 1) for 2 different wind speeds (5 and 10 m/s) and 4 different ML depths (10–40 m; the previous experiments without stratification can be considered as cases with ML deeper than 50 m). The stratification below the ML remains the same in all cases (temperature gradient of 7 °C/50 m) though almost any stratification tested would diminish the turbulent mixing below the ML; temperature was held constant throughout the simulations. In these experiments, it was found that the best comparison between the model and the Ekman calculation was obtained when the Ekman formula uses the mean KM over the imposed ML depth plus 10 m (i.e., including the upper thermocline below the ML). Imposing Ekman ML depth (D_E in Eq. 4c) regardless of KM did not improve the Ekman calculations, since it may be inconsistent with the surface currents which also depends on KM (V_0 in Eq. 4b). Of course, if observations exist for both D_E and V_0, one may try to impose them on the Ekman formula, but they may not be consistent with the actual depth-dependent KM.

Two examples from these experiments are shown in Fig. 8 and Fig. 9 for 10-m mixed layer depth and wind speed of 5 m/s and 10 m/s, respectively. The results show that the model's turbulence and currents are restricted to mostly within the mixed layer depth, while in the Ekman solution, currents decay much slower below the ML; this result is consistent with the observations in Price et al. (1987). Surface velocity speed and direction in the model are very similar to the Ekman solution, but in the model, the velocity abruptly turns and decays at the bottom of the ML between 10 and 20 m, while in the Ekman solution, currents decay more slowly down to ~ 30–40 m depth, as they are controlled by the Ekman layer depth D_E, independent of the actual ML depth.

A summary of the ML experiments shows the mean KM (Fig. 10a) and the velocity difference between the model and Ekman solutions (Fig. 10b), as a function of ML depth. The overall difference decreases with increasing ML depth, as the model is getting closure to the homogeneous Ekman solution. Based on Fig. 10a, an empirical relation was found that allows to predict the mean KM (in cm^2/s) to be used by the Ekman formula as a function of wind speed (U *in m/s*) and imposed model ML depth (D_M in m):

$$KM(model) = 0.38U + 0.132U^2 + 0.406UD_M - 0.46D_M. \quad (9)$$

While this empirical formula is most accurate for 5 m/s < U < 10 m/s, because of the almost linear nature of the results, it can likely be applied to 2 m/s < U < 15 m/s, as in Eq. 8. Note, however, that the KM in the Ekman equation (Eq. 4c) is connected to the Ekman layer depth D_E by a different relation:

$$KM(Ekman) = (f/2)(D_E/\pi)^2. \quad (10)$$

D_M in (9) can be used with observed ML depth resulted from surface heat fluxes, wind and wave mixing, and other turbulent processes in a stratified ocean, while D_E in (10) represents the theoretical wind-influenced Ekman depth in unstratified ocean. The two calculations are compared in Fig. 10a, showing that the theoretical Ekman depth for a given mixing is like the ML depth only for weak winds (~ 5 m/s) and deep ML (40–50 m); otherwise, the model mean KM is larger than the mixing implied by the Ekman theory. Figure 11 evaluates the accuracy of the empirical relation in Eq. (9) for the different cases of Fig. 10a, showing that for 5 m/s < U < 10 m/s and 10 m < D_M < 50 m, the correlation between the model results and the prediction of mean KM in Eq. (9) is statistically very significant ($R^2 = 0.98$, $p < 0.001$). While the empirical relations have not been tested for a wider range of factors, Eqs. (8) and (9) may provide a good estimate of KM to be used in the Ekman formula for homogeneous and for stratified oceans, respectively. The Ekman theory implies a relation between the Ekman depth and KM (10), but it does not provide any relation between wind stress (or wind velocity) and KM; therefore, an empirical relation such as Eq. (9) can fill this gap and allows more practical usage of the Ekman theory if the wind is observed.

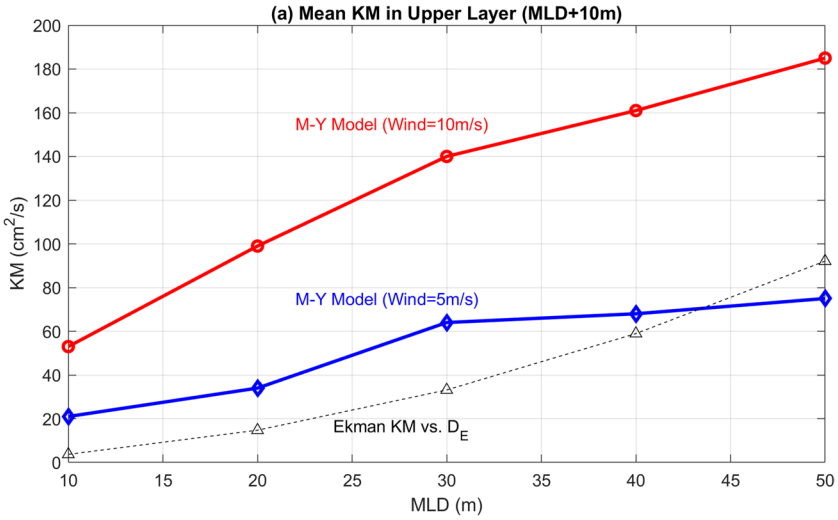

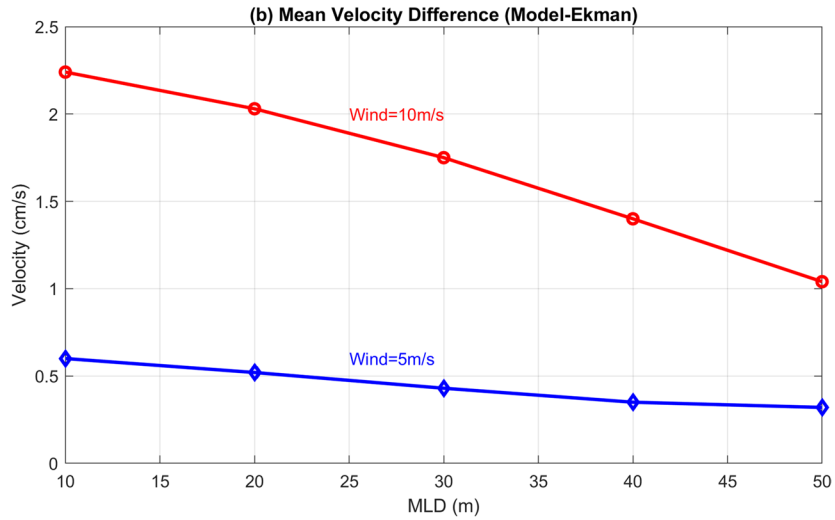

Fig. 10 Summary of the simulations with different model mixed layer depths (cases 3, 10, and 14–21 in Table 1); MLD = D_M in Eq. 9. **a** Mean model KM over the MLD + 10 m. **b** Mean velocity difference over the water column between the M-Y model and the Ekman solution. Results are shown for 5 m/s wind (blue) and 10 m/s wind (red). Also shown in Fig. 10a (dash line) is the KM derived from the Ekman depth D_E in Eq. 10

5 Summary and conclusions

The study addressed a very basic question in physical oceanography that has been of interest for over a century since the pioneering work of Ekman (1905) — how well can a simple theoretical model of wind-driven currents represent the (more complex) real ocean? The general concept that surface wind currents are proportional to wind stress, turn to the right in the northern hemisphere by the Coriolis force, and quickly decay with depth, has been observed many times. It is also well recognized that oceanic mixing in the upper layers is driven by turbulent and not molecular diffusion (though exact solution to turbulent motion is yet to be found). Observations also verified that the total Ekman transport of the upper layers is directed ~ 90° from the wind direction, as predicted by the Ekman theory, and its value is within ~ 10% of the theoretical Ekman transport (Price et al 1987). However, the observed change of currents

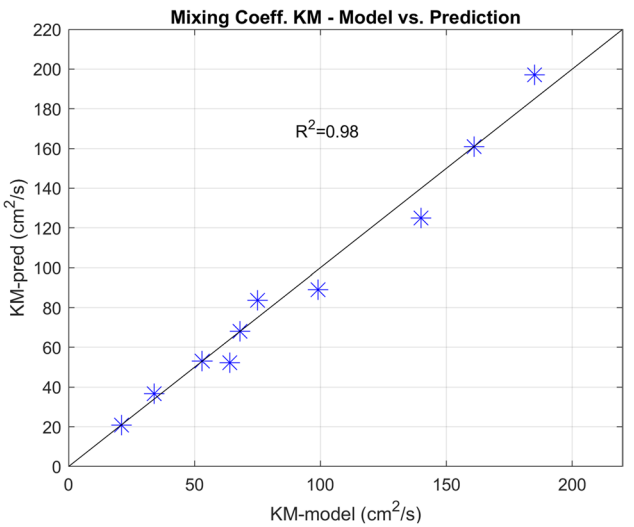

Fig. 11 A comparison between the mean model KM of Fig. 10a and the predicted KM from Eq. 9

with depth is often quite different than the classical Ekman spiral shown in textbooks (Pond and Pickard 1983; Mellor 1996). There are two main drawbacks of the Ekman solution. First, the ocean is not homogeneous but has stratification that affects mixing and changes spatially (e.g., different surface heat fluxes and winds at different latitudes) and temporally (e.g., seasonal mixed layer) (Ezer 2000). Second, the Ekman theory is based on the assumed balance between the Coriolis force and vertical mixing with a constant turbulent mixing coefficient, while the actual ocean turbulence can vary by several orders of magnitude under different conditions and at different depths; the turbulent mixing coefficient is usually unknown and rarely directly measured. It is also difficult to compare the Ekman theory with observations (Price et al 1987), because the ocean currents are rarely in a steady state and it is often difficult to separate wind-driven currents from other flows such as baroclinic geostrophic currents driven by density gradients, tidal-driven currents, or currents driven by interaction with changing topography.

Is the Ekman solution applicable to the real ocean despite the unrealistic assumptions of the Ekman theory? It provides a useful formula to estimate how ocean currents change with depth for a given latitude and wind stress — but only if specific constant KM is assumed. Therefore, this study aims to evaluate the accuracy of the theoretical Ekman solution and learn how the currents may change when the assumptions in the original theory are not met, such as when KM is a function of depth and when there is stratification with a mixed layer. To do that, a simple one-dimensional (1D) time-dependent numerical ocean model with the Mellor–Yamada turbulent scheme (Mellor and Yamada 1982) was used to generate turbulent mixing coefficients under different conditions and see how currents diverge from the classical Ekman solution. Moreover, the model is used as a practical tool to estimate the effective KM to be used by the Ekman formula under different conditions. This study follows a long tradition of 1D models used for studying oceanic mixing (Mellor and Durbin 1975; Huang 1979; Martin 1985; Price et al 1987; Gaspar et al. 1990; Mellor 2001; Mellor and Blumberg 2004). A systematic quantitative comparison was made between the 1D numerical model and the Ekman solution to better understand how the Ekman spiral is affected by KM and stratification.

In the first set of experiments, the model temperature and salinity were held as constants like the Ekman assumption and only the vertical mixing coefficient varied with depth due to the M-Y model under different wind speeds. These results show that if the Ekman solution uses the mean KM obtained by the 1D model for each wind case, the difference between the Ekman and the model calculations are quite small in most of the water column, except a larger difference near the surface (~2–5 m). When adding in the 1D-MY model, the Craig and Banner (1994) (C-B) turbulent boundary condition that induced mixing by surface breaking waves, the model surface current is more like the Ekman solution, especially for strong winds when large waves are expected. The Ekman formula (Eq. 4b) implies that the surface velocity is proportional to τ/KM, so having $KM \to 0$ when $z \to 0$ may result in too large surface velocity in the original M-Y model without waves. However, for practical purposes, in most cases, models and observations do not resolve the few centimeters to O(1 m) scales near the surface, so this is less of a problem.

In the second set of experiments, a mixed layer (ML) was added at different depths. It is assumed that the simulations conducted here represent short-term wind blowing over an existing ML (due to say seasonal heating and cooling), and not a ML evolved directly from the action of the wind (as in Fig. 1). In these cases, the stable stratification below the ML abruptly diminishes the turbulence and currents in the model, compared with the Ekman solution where the currents decay exponentially with depth, ignoring changes in density gradients (and Richardson number). However, it was found empirically that if the Ekman formula uses a mean KM calculated from the model over the imposed ML depth (plus 10 m, to represent the thermocline below the ML), the model and Ekman solutions are quite similar.

The study does not aim at comparisons with near-surface observations of small-scale turbulence, which is a very difficult task. Instead, it conducts high-resolution model simulations to test how the wind-driven current is affected by different factors such as wind speed, non-constant turbulent mixing, and stratification — evaluations of the differences between the classical Ekman theory and the ocean model thus shed light on the behavior of the Ekman currents. These sensitivity experiments followed the footsteps of past studies that tried to compare the Ekman spiral with observations but often were inconclusive and only qualitative (Price et al 1987). A practical result of the study was the finding of an empirical formula (9) that, given observed wind and mixed layer depth, can provide an estimate of the mean KM to be used by the Ekman formula (3), and thus allows one to calculate wind-driven velocities in the ocean without a numerical model. It is acknowledged that this empirical formula may not be accurate for all oceanic conditions, but since the turbulent mixing coefficient is largely unknown and can change by several orders of magnitude in space and time, the finding here provides an estimate of KM that is probably within observational errors.

Besides the contribution of this study to classical theories in physical oceanography, better understanding of turbulent processes in the upper ocean and the tools provided here to estimate turbulent mixing coefficients may also have implications for biological processes and ecosystem dynamics. For example, particulate organic carbon supplied to the mesopelagic zone from the upper ocean may involve turbulent processes such as the mixed layer biological pump (Dall'Olmo et al. 2016; Lacour et al 2019), and quantifying Ekman upwelling that contribute to biological productivity also involves turbulent processes (McClain and Firestone 1993; Jacox et al 2018). Since 1D models neglect horizontal

variations, they cannot capture horizontal advection, coastal Ekman upwelling, or Ekman pumping upwelling, so further studies of turbulence with 3D models, high-resolution observations, and theoretical frameworks are still needed.

Acknowledgements The Center for Coastal Physical Oceanography (CCPO) provided facility and computational resources. The author is also affiliated with ODU's Institute for Coastal Adaptation and Resilience (ICAR). Two anonymous reviewers are thanked for providing useful suggestions.

Data availability No external data were used in the study. The M-Y model code is publicly available at http://www.ccpo.odu.edu/POMWEB/.

Declarations

Conflict of interest The author declares no competing interests.

References

Beesley D, Olejarz J, Tandon A, Marshall J (2008) A laboratory demonstration of Coriolis effects on wind-driven ocean currents. Oceanography 21(2):72–76. https://www.jstor.org/stable/24805614

Blumberg AF, Mellor GL (1987) A description of a three-dimensional coastal ocean circulation model, Three-Dimensional Coastal Ocean Models, Coastal Estuarine Stud., 4:1–16, Heaps NS, AGU, Washington, D.C. https://doi.org/10.1029/CO004p0001

Choi Y, Noh Y, Hirose N, Song H (2022) Improvement of the ocean mixed layer model via large-eddy simulation and inverse estimation. J Atmos Oceanic Technol 39(10):1483–1498. https://doi.org/10.1175/JTECH-D-21-0157.1

Craig PD, Banner ML (1994) Modeling wave-enhanced turbulence in the ocean surface layer. J Phys Oceanogr 24:2546–2559. https://doi.org/10.1175/1520-0485(1994)024%3c2546:MWETIT%3e2.0.CO;2

Dall'Olmo G, Dingle J, Polimene L, Brewin RJW, Claustre H (2016) Substantial energy input to the mesopelagic ecosystem from the seasonal mixed-layer pump. Nat Geosci 9. https://doi.org/10.1038/NGEO2818

Ekman VW (1905) On the influence of the earth's rotation on oceancurrents. Ark Math Astron Fys 2:1–53

Ezer T (2000) On the seasonal mixed-layer simulated by a basin-scale ocean model and the Mellor Yamada turbulence scheme. J Geophys Res 105(C7):16843–16855. https://doi.org/10.1029/2000JC900088

Ezer T (2005) Entrainment, diapycnal mixing and transport in three-dimensional bottom gravity current simulations using the Mellor-Yamada turbulence scheme. Ocean Model 9(2):151–168. https://doi.org/10.1016/j.ocemod.2004.06.001

Galperin B, Kantha LH, Hassid S, Rosati A (1988) A quasi-equilibrium turbulent energy model for geophysical flows. J Atmos Sci 45:55–62

Garratt JR (1977) Review of drag coefficients over oceans and continents. Mon Wea Rev 105:915–929. https://doi.org/10.1175/1520-0493(1977)105%3c0915:RODCOO%3e2.0.CO;2

Gaspar P, Grégoris Y, Lefevre JM (1990) A simple eddy kinetic energy model for simulations of the oceanic vertical mixing: tests at station Papa and long-term upper ocean study site. J Geophys Res 95(C9):16179–16193. https://doi.org/10.1029/JC095iC09p16179

Hu H, Wang J (2010) Modeling effects of tidal and wave mixing on circulation and thermohaline structures in the Bering Sea: process studies. J Geophys Res 115(C1). https://doi.org/10.1029/2008JC005175

Huang NE (1979) On surface drift currents in the ocean. J Fluid Mech 91(1):191–208. https://doi.org/10.1017/S0022112079000112

Huang CJ, Qiao F, Song Z, Ezer T (2011) Improving simulations of the upper-ocean by inclusion of surface waves in the Mellor-Yamada turbulence scheme. J Geophys Res 116(C1007). https://doi.org/10.1029/2010JC006320

Jacox MG, Edwards CA, Hazen EL, Bograd SJ (2018) Coastal upwelling revisited: Ekman, Bakun, and improved upwelling indices for the US West Coast. J Geophys Res 123(10):7332–7350. https://doi.org/10.1029/2018JC014187

Lacour L, Briggs N, Claustre H, Ardyna M, Dall'Olmo G (2019) The intraseasonal dynamics of the mixed layer pump in the subpolar North Atlantic Ocean: a biogeochemical-Argo float approach. Global Biogeochem Cyc 33:266–281. https://doi.org/10.1029/2018GB005997

Martin PJ (1985) Simulation of the mixed layer at OWS November and Papa with several models. J Geophys Res 90:903–916. https://doi.org/10.1029/JC090iC01p00903

McClain CR, Firestone J (1993) An investigation of Ekman upwelling in the North Atlantic. J Geophys Res 98(C7):12327–12339. https://doi.org/10.1029/93JC00868

Mellor GL (1996) Introduction to physical oceanograhy. American Institute of Physics, Melville, p 260. https://link.springer.com/book/9781563962103

Mellor GL (2001) One-dimensional, ocean surface layer modeling: a problem and a solution. J Phys Oceanogr 31:790–809. https://doi.org/10.1175/1520-0485(2001)031%3c0790:ODOSLM%3e2.0.CO;2

Mellor GL, Blumberg A (2004) Wave breaking and ocean surface layer thermal response. J Phys Oceanog 34(3):693–698. https://doi.org/10.1175/2517.1

Mellor GL, Durbin PA (1975) The structure and dynamics of the ocean surface mixed layer. J Phys Oceanog 5:718–728. https://doi.org/10.1175/1520-0485(1975)005%3c0718:TSADOT%3e2.0.CO;2

Mellor GL, Yamada T (1982) Development of a turbulent closure model for geophysical fluid problems. Rev Geophys 20:851–875. https://doi.org/10.1029/RG020i004p00851

Munk WH (1950) On the wind-driven ocean circulation. J Atmos Sci 7(2):80–93. https://doi.org/10.1175/1520-0469(1950)007%3c0080:OTWDOC%3e2.0.CO;2

Noh Y, Kim HJ (1999) Simulation of temperature and turbulence structure of the oceanic boundary layer with the improved near-surface process. J Geophys Res 104:15621–15634. https://doi.org/10.1029/1999JC900068

Pond S, Pickard GL (1983) Introductory Dynamical Oceanography, 2nd edn. Elsevier, Oxford, p 329

Price JF, Weller RA, Schudlich RR (1987) Wind-driven ocean currents and Ekman transport. Science 238:1534–1538. https://doi.org/10.1126/science.238.4833.1534

Stacey MW, Pond S (1997) On the Mellor-Yamada turbulence closure scheme: the surface boundary conditions for q2. J Phys Oceanogr 27:2081–2086. https://doi.org/10.1175/1520-0485(1997)027%3c2081:OTMYTC%3e2.0.CO;2

Wang J, Ikeda M, Saucier F (2003) A theoretical, two-layer, reduced-gravity model for descending dense water flow on continental slopes. J Geophys Res 108(C5). https://doi.org/10.1029/2000JC000517